



A new form of vanadium oxide for use as a cathode material in lithium batteries

Jinxiang Dai^a, Sam F.Y. Li^{b,*}, Zhiqiang Gao^a, Kok Siong Siow^a

^a Department of Chemistry, National University of Singapore, 10 Kent Ridge Crescent, Singapore 119260, Singapore

^b Department of Chemistry and Institute of Material Research and Engineering, National University of Singapore, 10 Kent Ridge Crescent, Singapore 119260, Singapore

Received 18 August 1997; accepted 16 December 1997

Abstract

A new form of vanadium oxide, $(\text{Na}_2\text{O})_{0.23}\text{V}_2\text{O}_5$, is synthesised by precipitation of sol and removing water. Its performance as a cathode material is studied by chronopotentiometry and cyclic voltammetry. A capacity of more than 220 mA h g^{-1} can be obtained in 12 cycles when the voltage is from 3.8 to 1.8 V. Its capacity and cyclability are satisfactory in comparison with other forms of vanadium oxide and synthesis is relatively easy. X-ray diffraction (XRD) studies show that $(\text{Na}_2\text{O})_{0.23}\text{V}_2\text{O}_5$ is quasi-tetragonal crystal after heating at a temperature below 250°C . The crystallites of $(\text{Na}_2\text{O})_{0.23}\text{V}_2\text{O}_5$ are in platelet form, and their dimensions are less than $2 \mu\text{m}$. Thermogravimetric analysis (TGA) and differential scanning calorimetry (DSC) studies found that the sol-precipitate, $(\text{Na}_2\text{O})_{0.23}\text{V}_2\text{O}_5 \cdot x\text{H}_2\text{O}$, can lose water at 200°C . © 1998 Elsevier Science S.A. All rights reserved.

Keywords: Lithium batteries; Cathode materials; Vanadium oxide

1. Introduction

Many forms of vanadium oxide have been studied as cathode materials for lithium batteries [1–7], especially when a polymer is used as the electrolyte. Crystal vanadium oxide ($\text{c-V}_2\text{O}_5$) when used as such a cathode material exhibits poor rechargeability and unsatisfactory voltage regulation because of changing crystallinity during discharge–charge cycles [1–3]. Types of amorphous vanadium oxide ($\text{a-V}_2\text{O}_5$), such as $\text{V}_2\text{O}_5\text{–P}_2\text{O}_5$, $\text{V}_2\text{O}_5\text{–TiO}_2$, $\text{V}_2\text{O}_5\text{–TeO}_2$, have been studied as cathode materials for use in lithium batteries [4,6,8]. By comparison with $\text{c-V}_2\text{O}_5$, they are more satisfactory in terms of rechargeability, voltage regulation and reversible intercalated lithium value per mole V_2O_5 ($\times F/\text{mol V}_2\text{O}_5$). Obviously, their specific capacities will decrease if the weight of the inert ingredients such as P_2O_5 , TiO_2 , TeO_2 is considered. Recently, V_2O_5 xerogel ($\text{XRG-V}_2\text{O}_5$) was studied as a cathode material [7]. It is an amorphous form of V_2O_5 synthesised by a sol–gel method. $\text{XRG-V}_2\text{O}_5$ has a larger specific capacity

than $\text{a-V}_2\text{O}_5$. β -Bronze, $\text{Na}_x\text{V}_2\text{O}_5$, is a form of monoclinic crystal oxide that has been used as a cathode material [9,10], and can be obtained by annealing Na^+ -ion exchanged product from $\text{XRG-V}_2\text{O}_5$ at 550°C . In this study we have synthesised a new form of vanadium oxide, $(\text{Na}_2\text{O})_{0.23}\text{V}_2\text{O}_5$, by precipitation of sol and removal of water. Its performance as a cathode material is studied by chronopotentiometry and cyclic voltammetry.

2. Experimental

The $(\text{Na}_2\text{O})_{0.23}\text{V}_2\text{O}_5 \cdot x\text{H}_2\text{O}$ was synthesized by refluxing a sol of V_2O_5 . The latter was produced according to the method described by Lemerle et al. [10], except that the solution of NaVO_3 was acidified by adding an acid solution instead of a proton exchanging resin. After precipitation from the V_2O_5 sol, the product was washed with water and filtered. The resulting $(\text{Na}_2\text{O})_{0.23}\text{V}_2\text{O}_5 \cdot x\text{H}_2\text{O}$ could be used as cathode material after removal of water at 250°C for 10 h. The composition of the product was analyzed with atomic absorption spectrophotometry (AAS), inductive coupled plasma, atomic emission spectrophotometry (ICP-AES) and X-ray fluorescence (XRF). The sol-

* Corresponding author.

precipitated sample was used in TGA and DSC experiments after being dried at 120°C in a vacuum oven. The TGA and DSC measurements were performed in air. XRD patterns were obtained using a Philips PW 1729 X-ray powder diffractometer. X-ray profiles were measured between 5 to 60° using a monochromatized $\text{CuK}\alpha$ radiation source ($\lambda = 1.5418 \text{ \AA}$). The morphology of the samples was examined with a JEOL-JSM35CF scanning electron microscope.

The composite cathode electrode materials were prepared from active material, carbon black and polytetrafluoroethylene (PTFE) binder. The cathodes were made by pressing the composite cathode electrode material on to an aluminium disc at a pressure of 2.4 Torr cm^{-2} . The electrode diameter was 18 mm. The anodes were lithium foils pressed on nickel discs. The cathodes, polyethylene separators, and anodes were assembled in a sandwich structure. Cyclic voltammetry was performed on flooded cells. The electrolyte was prepared by dissolving LiClO_4 in blended EC and DMC. The concentration of LiClO_4 was 1.0 M, and the volumetric ratio of EC:DMC was 1:1.

3. Results and discussion

3.1. TGA and DSC analysis

The $(\text{Na}_2\text{O})_{0.23}\text{V}_2\text{O}_5 \cdot x\text{H}_2\text{O}$ dried at 120°C typically contained 6.95 wt.% water, as shown in Fig. 1. This proportion of water corresponded to $x = 0.814$. The water is lost at 190–200°C, as shown by DSC and TGA. TGA shows that the sample treated at 250°C is stable up to 700°C. This indicates that the water can be removed completely if the sample is treated at 250°C for 10 h.

3.2. X-ray diffraction

XRD patterns of samples are reported in Fig. 2. They are similar to that for $\beta\text{-V}_2\text{O}_5$ [11], and belong to the tetragonal crystal system. The $(\text{Na}_2\text{O})_{0.23}\text{V}_2\text{O}_5 \cdot x\text{H}_2\text{O}$ treated at 120°C is poorly crystalline, as indicated by lower peak intensity. The 200 peak is found at $2\theta = 11.840^\circ$, corresponding to $d = 7.468 \text{ \AA}$ and $a = 14.937 \text{ \AA}$. Other samples treated at temperature 250°C have 200 peaks at $2\theta = 12.8^\circ$, corresponding to $d = 6.90 \text{ \AA}$ and $a = 13.88 \text{ \AA}$. This is caused by water loss. The crystallinity of the samples becomes perfect at temperature above 450°C. In contrast, poor crystallinity is maintained at 250°C. The peak intensity is the same as that of a sample treated at 120°C, but the peak position is identical to that of a sample treated at 450°C. The $(\text{Na}_2\text{O})_{0.23}\text{V}_2\text{O}_5 \cdot x\text{H}_2\text{O}$ can lose water and maintain the quasi-crystalline state after heating at 250°C for 10 h. This result agrees with the TGA and DSC results.

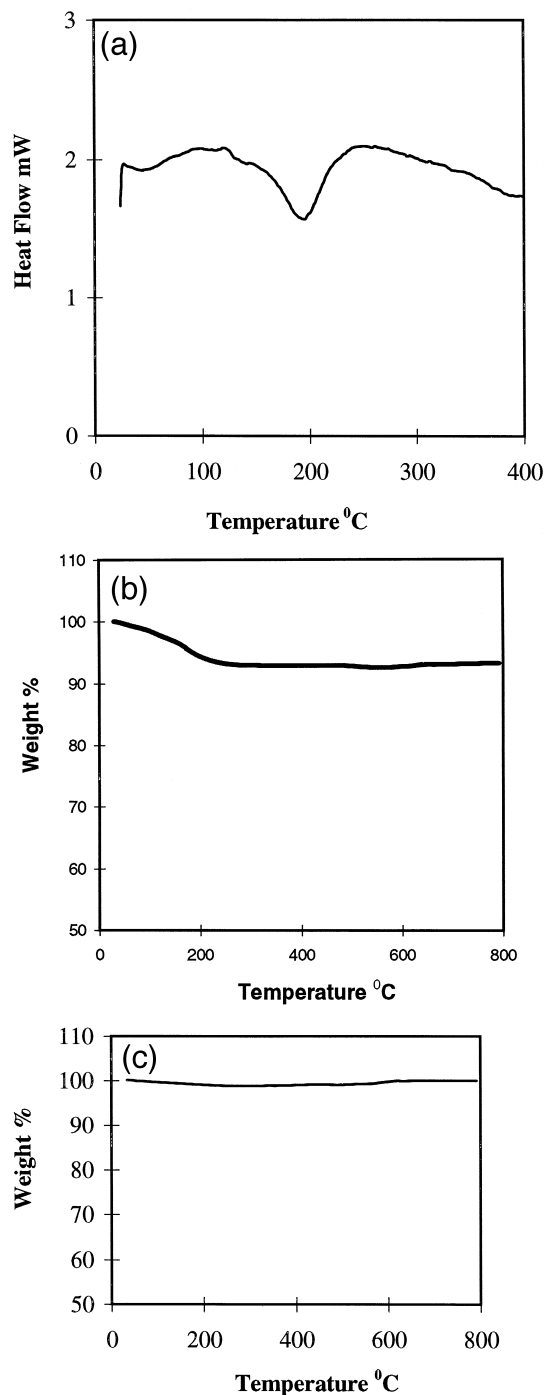


Fig. 1. DSC and TGA curves of $(\text{Na}_2\text{O})_{0.23}\text{V}_2\text{O}_5 \cdot x\text{H}_2\text{O}$. (a) DSC of the sample treated at 120°C, 5°C min^{-1} , in air; (b) TGA of sample treated at 120°C, 5°C min^{-1} , in air; (c) TGA of sample treated at 250°C, $10^\circ\text{C min}^{-1}$, in air.

3.3. Electrochemical performance

The electrochemical behaviour of the sample heated at 250°C in a galvanostatic mode is illustrated in Fig. 3. The characteristic voltage curve displays a single step for Li insertion around 2.4 V with a first discharge capacity of 270 mA h g^{-1} when 1.7 V is selected as the cut-off

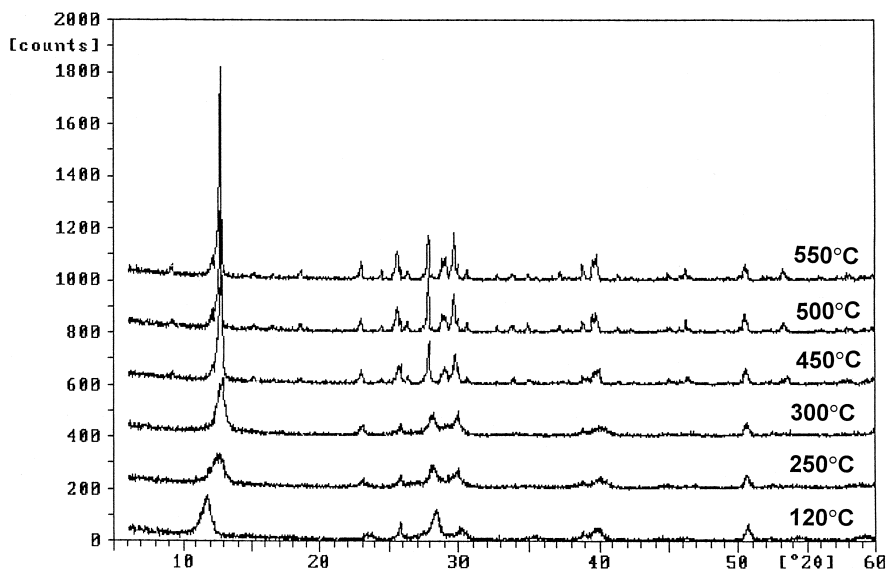


Fig. 2. XRD patterns of the samples treated at different temperatures.

voltage. The first discharge capacity is equal to a faradaic yield of $1.98F/\text{mol}$ and corresponds to the quasi-quantitative reduction of V^{5+} ions to V^{4+} ions. This value is higher than that of XRG V_2O_5 , 250 mA h g^{-1} equal to a faradaic yield of $1.8F/\text{mol}$ [12]. However, the voltage is lower than that of XRG V_2O_5 . This may be caused by higher current density, $100 \mu\text{A cm}^{-2}$, and the lower conductivity of $(\text{Na}_2\text{O})_{0.23}\text{V}_2\text{O}_5$. The large voltage difference between the discharge and the charge curve is due to the poor conductivity of $(\text{Na}_2\text{O})_{0.23}\text{V}_2\text{O}_5$. The performance over 12 cycles is shown in Fig. 4. The $(\text{Na}_2\text{O})_{0.23}\text{V}_2\text{O}_5$ is cyclable when the capacity is 220 mA h g^{-1} , corresponding to $1.61F/\text{mol}$. The capacity is over 220 mA h g^{-1} after 12 cycles.

The electrochemical characteristics of the sample treated at 250°C were evaluated from the cyclic voltammetric study shown in Fig. 5. The single oxidizing step is verified

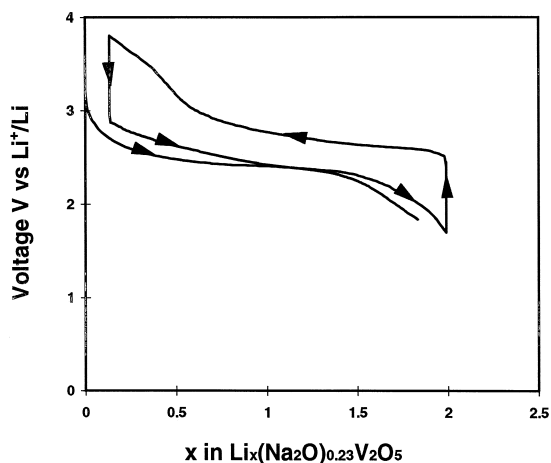


Fig. 3. Cyclic characteristics of $(\text{Na}_2\text{O})_{0.23}\text{V}_2\text{O}_5$ as a cathode material; current density: $100 \mu\text{A cm}^{-2}$.

by the single broad anode peak at 2.8 V . The single cathode peak at 2.3 V and the two shoulders at 2.6 and 2.8 V show that the multi-reducing steps merge, and cannot be divided clearly. This result indicates that there are no structural changes during the lithium intercalating and de-intercalating process.

The discharge–charge curves of $(\text{Na}_2\text{O})_{0.23}\text{V}_2\text{O}_5$ annealed at 450°C , and the discharge curves of $(\text{Na}_2\text{O})_{0.23}\text{V}_2\text{O}_5$ annealed at 500°C are given in Figs. 6 and 7, respectively. From Fig. 6, it is seen that the capacity is less than 180 mA h g^{-1} and the cyclability is poor. The data in Fig. 7 show that the capacity of the sample annealed at 500°C is $\sim 150 \text{ mA h g}^{-1}$, and after 3 cycles, the capacity decreases less than to 60 mA h g^{-1} . The

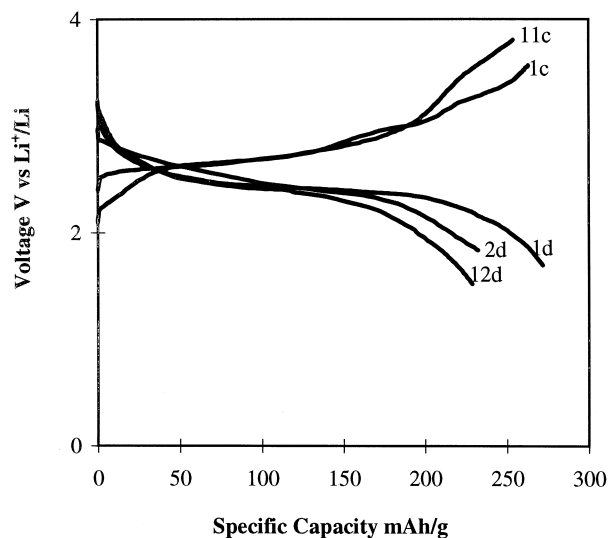


Fig. 4. Discharge–charge curves of battery with $(\text{Na}_2\text{O})_{0.23}\text{V}_2\text{O}_5$; current density: $100 \mu\text{A cm}^{-2}$. n_c represents n th charging and n_d represents n th discharging.

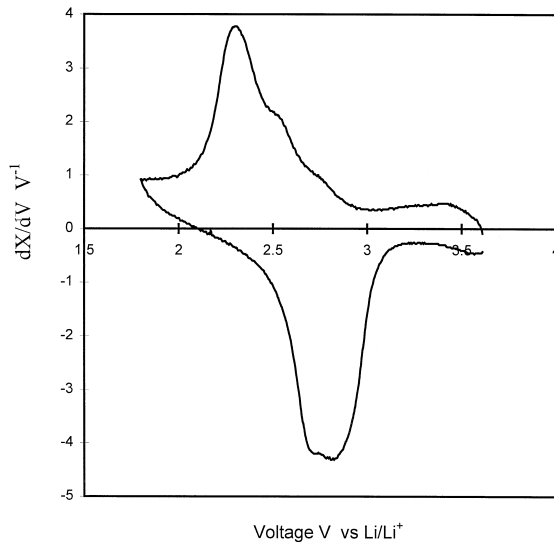


Fig. 5. Cyclic voltammety of flooded cell with $(\text{Na}_2\text{O})_{0.23}\text{V}_2\text{O}_5$.

results indicate that the perfect tetragonal crystal $(\text{Na}_2\text{O})_{0.23}\text{V}_2\text{O}_5$ exhibits poor electrochemical performance as a cathode material.

3.4. SEM

The morphologies of $(\text{Na}_2\text{O})_{0.23}\text{V}_2\text{O}_5$ annealed at different temperatures are illustrated by electron micrographs in Fig. 8. The crystallite form changes with treatment temperature. Samples treated at 120 and 250°C have a similar crystal structure, the crystallites consist of platelets of length less than 2 μm and width less than 0.4 μm .

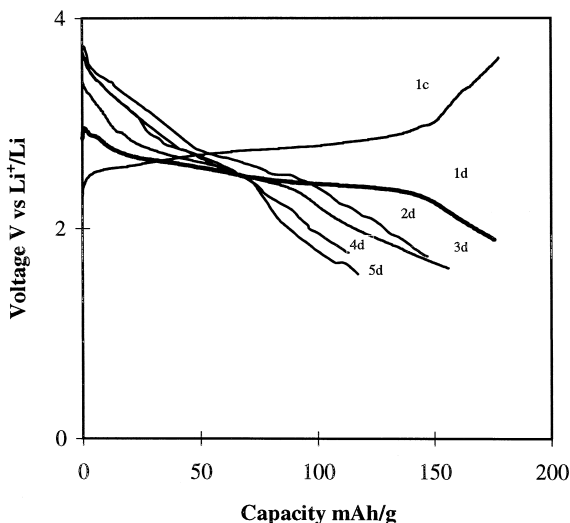


Fig. 6. Discharge-charge curves of battery with $(\text{Na}_2\text{O})_{0.23}\text{V}_2\text{O}_5$ annealed at 450°C as cathode material, 1c represents 1st charge and n_d represents n th discharge.

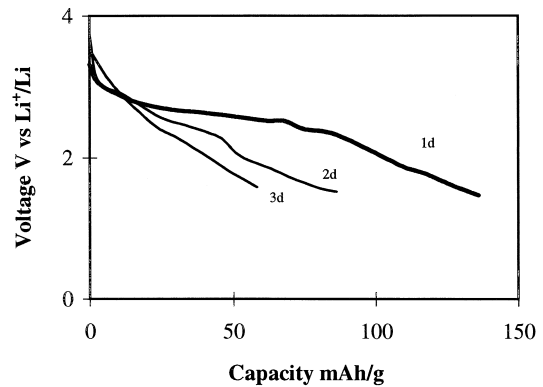


Fig. 7. Discharge curves of battery with $(\text{Na}_2\text{O})_{0.23}\text{V}_2\text{O}_5$ annealed at 500°C as cathode material n_d represents n th discharge.

Samples annealed at 350 and 450°C have a similar structure, the crystallites are again platelets, but of a size that is larger than that of the 120 and 250°C samples. The crystallite size increases with treatment temperature. The crystallites of the 500 and 550°C samples are larger hexahedrons with square faces. The longer sides of the faces are up to several μm in length, and the shorter sides are less than 1 μm . This morphological study reveals that the samples change to a perfect crystal structure after annealing at temperatures over 450°C. This finding agrees with the X-ray results. The imperfect crystallites of samples treated at a temperature below 250°C have larger surface area and a more flexible morphology. This results in larger capacity and better cyclability as cathode materials [13].

3.5. IR results

The IR spectra of $c\text{-V}_2\text{O}_5$ and $(\text{Na}_2\text{O})_{0.23}\text{V}_2\text{O}_5$ annealed at different temperatures is presented in Fig. 9. For $(\text{Na}_2\text{O})_{0.23}\text{V}_2\text{O}_5$ annealed at 450 and 500°C, the peaks indicate the double bond $\text{V}=\text{O}$ at 1011 cm^{-1} (in V_2O_5) divided into triple peaks. For $(\text{Na}_2\text{O})_{0.23}\text{V}_2\text{O}_5$ annealed at 450°C, the $\text{V}=\text{O}$ triple peaks are at 957.8, 979.0 and 1003.1 cm^{-1} . For the sample annealed at 500°C, the peaks are at 955.8, 973.2 and 998.3 cm^{-1} . This result suggests that $\text{V}=\text{O}$ in $(\text{Na}_2\text{O})_{0.23}\text{V}_2\text{O}_5$ is different from that in $c\text{-V}_2\text{O}_5$. The breaking of the $\text{V}=\text{O}$ double bond may be caused by the different position of $\text{V}=\text{O}$ in the crystal cell. Samples with a poorly crystalline state (e.g., those treated at 120 and 250°C) have the $\text{V}=\text{O}$ double bond peak divided into four peaks, at 948.1, 962.6, 1005.03 and 1017.6 cm^{-1} for the 120°C sample, and 955.8, 977.1, 100.2 and 1026.2 cm^{-1} for the 250°C sample. These features show that the $(\text{Na}_2\text{O})_{0.23}\text{V}_2\text{O}_5$ is very different in structure from amorphous $18\text{TiO}_2 \cdot 82\text{V}_2\text{O}_5$, $\text{V}_2\text{O}_5 \cdot \text{P}_2\text{O}_5$, $15\text{Li}_2\text{O} \cdot 85\text{V}_2\text{O}_5$ and gel- V_2O_5 with one $\text{V}=\text{O}$ peak similar to that for $c\text{-V}_2\text{O}_5$ [4,6,8]. The $\text{V}-\text{O}$ vibration peaks shifted from 810.3 cm^{-1} ($c\text{-V}_2\text{O}_5$) to 720.5, 743.6, 752.3

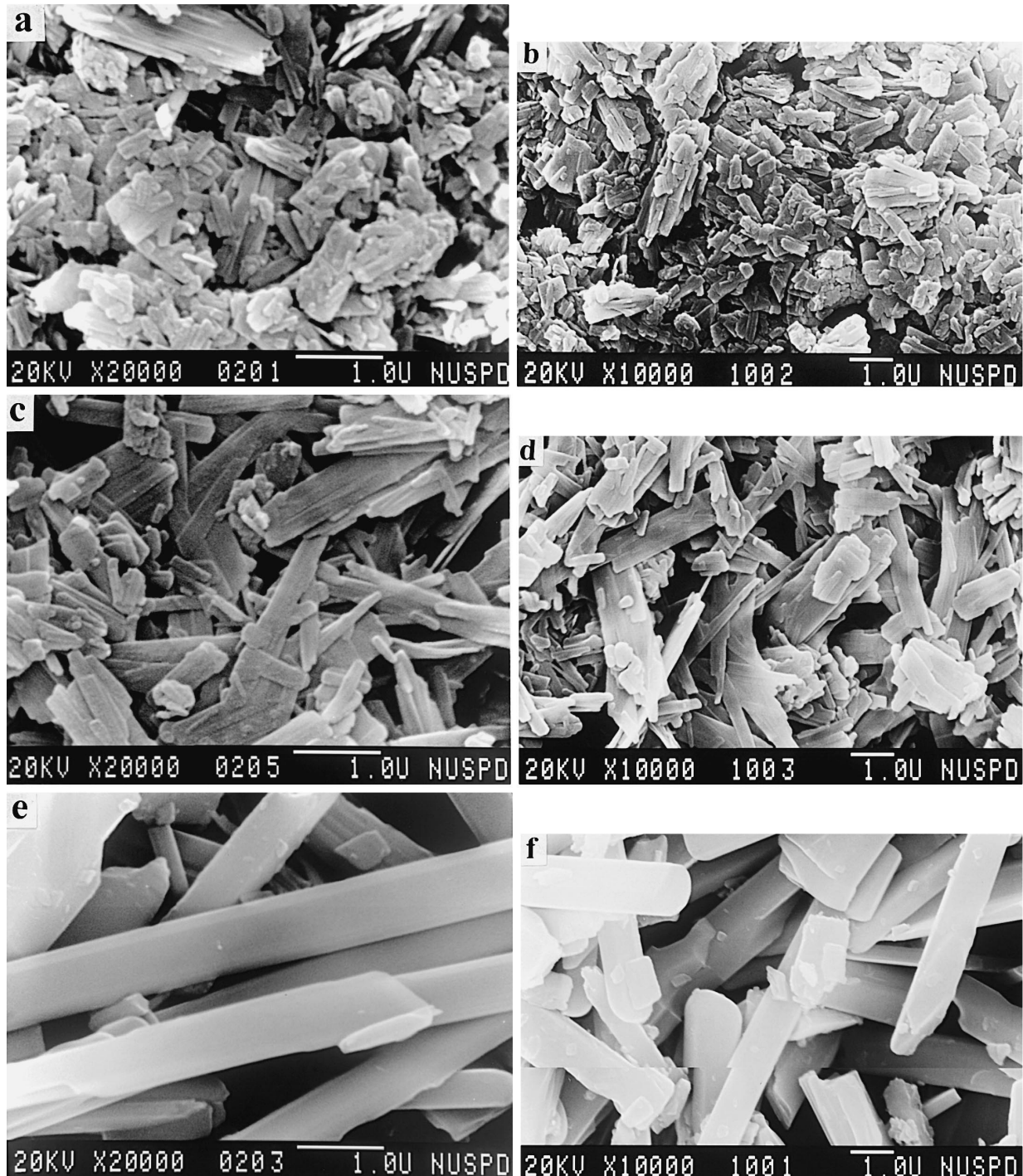


Fig. 8. Electron micrographs of samples annealed at different temperatures: (a) 120°C; (b) 250°C; (c) 350°C; (d) 450°C; (e) 500°C; (f) 550°C.

and 767.8 cm^{-1} for samples treated at 120, 250, 450 and 500°C, respectively. Another V–O bond peak has a similar shift in comparison with $c\text{-V}_2\text{O}_5$, from 588.4 to 539.2 cm^{-1} for the 120°C sample, and all samples treated at different temperatures have this peak at almost the same position. The change of quadruple-peaks to triple-peaks of the V=O double bond is most likely caused by a structural change from poorly crystalline samples treated at temperatures below 450°C to highly crystalline samples annealed

at temperatures above 450°C. This result can be verified by XRD results and electron micrographs.

4. Conclusions

A new form of vanadium oxide expressed by $(\text{Na}_2\text{O})_{0.23}\text{V}_2\text{O}_5 \cdot x\text{H}_2\text{O}$, is made by precipitation in sol produced from NaVO_3 solution by acidifying. The sample

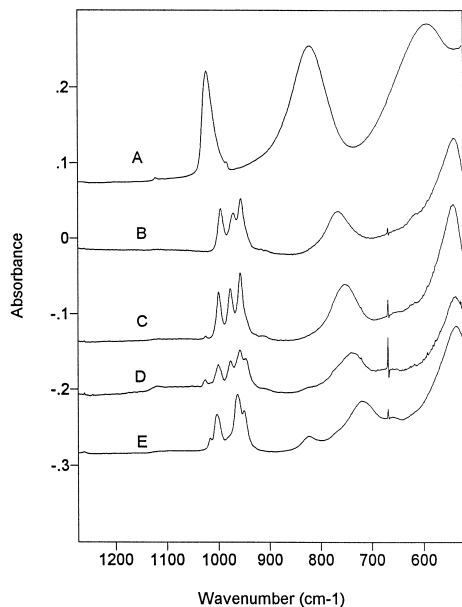


Fig. 9. IR curves of sample treated at different temperatures: (A) c- V_2O_5 ; (B) 550°C sample; (C) 450°C sample; (D) 250°C sample; (E) 120°C sample.

can lose water completely after heating at 250°C for 10 h. The $(Na_2O)_{0.23}V_2O_5$ can intercalate 1.98 mol of Li per mole formula, and displays good reversibility at 1.61 Li

per formula. It is a promising cathode material for lithium secondary batteries. The structure of $(Na_2O)_{0.23}V_2O_5$ annealed at different temperatures has been characterized by XRD, IR and SEM.

References

- [1] J.M. Cocciantell, M. Broussely, J.P. Doumerc, J. Labat, M. Pouchard, *J. Power Sources* 34 (1991) 103.
- [2] S. Okada, J. Yamaki, 176th Meeting of the Electrochem. Soc., Ext. Abs., Hollywood, 15–20 October, 1989, p. 62.
- [3] J.M. Cocciantell, M. Menetrier, C. Delmas, J.P. Doumerc, M. Pouchard, M. Broussely, J. Labat, *Solid State Ionics* 78 (1995) 143–150.
- [4] Y. Sakurai, J.-I. Yamaki, *J. Electrochem. Soc.* 135 (1988) 791–796.
- [5] M.G. Minett, J.R. Owen, *J. Power Sources* 32 (1990) 81–97.
- [6] T. Hirai, S. Okada, J.-I. Yamaki, *J. Electrochem. Soc.* 136 (1989) 3163–3169.
- [7] K. West, B. Zachai-Christiansen, M.J.L. Ostergard, T. Jacobsen, *J. Power Sources* 20 (1987) 165–172.
- [8] H. Hirashima, S. Kamimura, R. Muratake, T. Yoshida, *J. Non-Cryst. Solids* 100 (1988) 394–398.
- [9] J.P. Pereira-Ramos, R. Messina, L. Znaidi, N. Baffier, *Solid State Ionics* 28–30 (1988) 886–894.
- [10] J. Lemerle, L. Nejem, J. Lefebvre, *J. Chem. Res.* (1978) 5301.
- [11] JCPDS, 45–1074.
- [12] R. Baddour, J.P. Pereira-Ramos, R. Messina, J. Perichon, *J. Electroanal. Chem.* 314 (1991) 81.
- [13] J.P. Pereira-Ramos, N. Baffier, G. Pistoia, in: G. Pistoia (Ed.), *Lithium Batteries*, Elsevier, Amsterdam, 1994, pp. 298, 318.